

Unaltered reversible magnetic transition in Fe nanostructures upon ambient exposure

A. Quesada^{1*}, R. Gargallo-Caballero², Y. Montaña², M. Foerster³, L. Aballe³, J.F. Fernández¹, J. de la Figuera²

¹*Instituto de Cerámica y Vidrio (CSIC), Madrid 28049 (Spain)*

²*Instituto de Química Física “Rocasolano” (CSIC), Madrid 28006 (Spain)*

³*Alba Synchrotron Light Facility, CELLS, Barcelona 08290 (Spain)*

Abstract

High aspect-ratio Fe nanostrips are known to reversibly switch from a single-domain magnetic state to a multidomain diamond pattern as a function of temperature (T) and width. This magnetic bistability can be understood by the temperature-dependent balance between magnetocrystalline, shape and magnetoelastic anisotropies and has potential applications in magnetic logic devices. However, as Fe nanostructures easily oxidize, protecting the surface with capping layers may be required, which could largely affect the anisotropy balance. Here, we employ x-ray magnetic circular dichroism-photoemission electron microscopy (XMCD-PEEM) to study these thin Fe nanostrips before and after exposure to air.

Keywords: nanomagnetism; magnetic domains; transitions

*author to whom correspondence should be addressed: a.quesada@icv.csic.es

1. Introduction.

Magnetism is a thriving topic, fueled partly by current and future applications in information storage.[1,2] A great deal of innovative developments in the field are based on magnetic mesoscopic structures where new effects and means of control of magnetic properties blossom.[3–5] Metallic thin-films constitute in particular a fascinating and dynamic field, although they often bring about the technological challenge of preventing gas adsorption processes that could damage or alter their properties.[6,7] In mesoscopic magnetic systems, it is common that a subtle balance of anisotropies regulates the effect or functionality of interest and the use of capping layers or embedding the magnetic film in a multilayer can largely affect this balance.[8]

Recently, a reversible switching between two magnetic states was observed in epitaxial Fe nanostrips on Ru(0001).[9] These Fe nanostructures undergo a transition between single and multi-domain magnetic configurations as a function of temperature, an effect that was proven to be related to the temperature dependence of the different anisotropy terms/contributions, especially the magnetoelastic anisotropy originated by the mismatch with the Ru (0001) substrate. This bistability presents interesting opportunities in memory and logic device development; however, its applicability is limited by the fact that it has, so far, only been observed in an ultrahigh vacuum environment. The survival of this transition upon capping the nanostrips with a protective layer or upon exposure to air remains to be demonstrated.

In this work, we study the transition between single and multi-domain magnetic domain configurations in epitaxially grown Fe nanostrips before and after the exposure to

air, proving the robustness of the transition and monitoring the degree of oxidation using X-ray absorption spectroscopy (XAS) and x-ray magnetic circular dichroism (XMCD) both in combination with a photoemission electron microscope (PEEM).

2. Material and Methods

The experiments have been performed at the CIRCE beamline of the ALBA Synchrotron Light Facility. The beamline employs an Elmitec spectroscopic and low-energy electron microscope (SPELEEM).[10] The instrument allows acquiring either x-ray circular magnetic dichroism (XMCD) images to map the in-plane magnetization component along the x-ray direction with nanometer resolution, or selected area XMCD spectra as a function of photon energy. For XMCD images, images at the Fe L_3 -edge were taken with opposite photon helicity, subtracted pixel-by-pixel and divided by their sum. For the qualitative evaluation of the pixel intensity asymmetry shown in Fig. 3, the brightest/darkest pixel in Fig. 2 was arbitrarily determined to have an asymmetry of +0.5/-0.5 respectively. Local XMCD spectra are extracted from selected regions in XAS image stacks with varying photon energy, using opposite domains at constant helicity. The main microscope chamber operates as a molecular beam-epitaxy station with a base pressure below 1.10^{-10} mbar. Ru substrates were cleaned by annealing at 1400 K under 5.10^{-8} mbar O_2 . Eight atomic layers (AL) of Fe were deposited by molecular beam epitaxy onto clean Ru(0001) substrates in 1.10^{-6} mbar O_2 . The iron dose rate was 2 AL per minute and the substrate was kept at 920 K, which leads to the formation of Fe nanostrips on the surface. After growth, the samples were cooled down to room temperature in ultrahigh-vacuum (no O_2 atmosphere). Growth is monitored in real time and real space by low-energy electron

microscopy (LEEM). We study the properties of the nanostrips using XMCD-PEEM, XAS and LEEM before and after exposing the sample to air for 30 minutes.

3. Results.

Fig. 1 shows an XMCD-PEEM image at room-temperature (RT) of the sample, obtained at the Fe L_3 -edge in the initial state, i.e. after cooling from the growth temperature of 920 K in UHV. The resulting film is composed of Fe nanostrips and magnetite (Fe_3O_4) islands of triangular and trapezoidal shape, both on top of a FeO bilayer.[9] The FeO wetting layer shows no magnetic contrast, while both the Fe_3O_4 and Fe nanostructures present magnetic domains at RT. In particular, the result from our previous work is reproduced in that, depending on their width, Fe strips can be found in one of two magnetic states: essentially homogeneous single-domain states or multi-domain diamond states.[9] The specific domain structure of the diamond state is schematized in Fig. 1. Given that in XMCD-PEEM grayscale magnetic contrast is proportional to the magnetization vector along the photon beam direction, the nanostrips close to parallel/perpendicular orientation with respect to **the** beam reveal the four different domains in either four (upper right strip “1”, where red and green as well as blue and yellow domains are almost equivalent) or three (left lower strip “2”, red and yellow domain are equivalent) intensities respectively. A third strip “3” at the right edge was found to be in a single domain state (white) at RT.

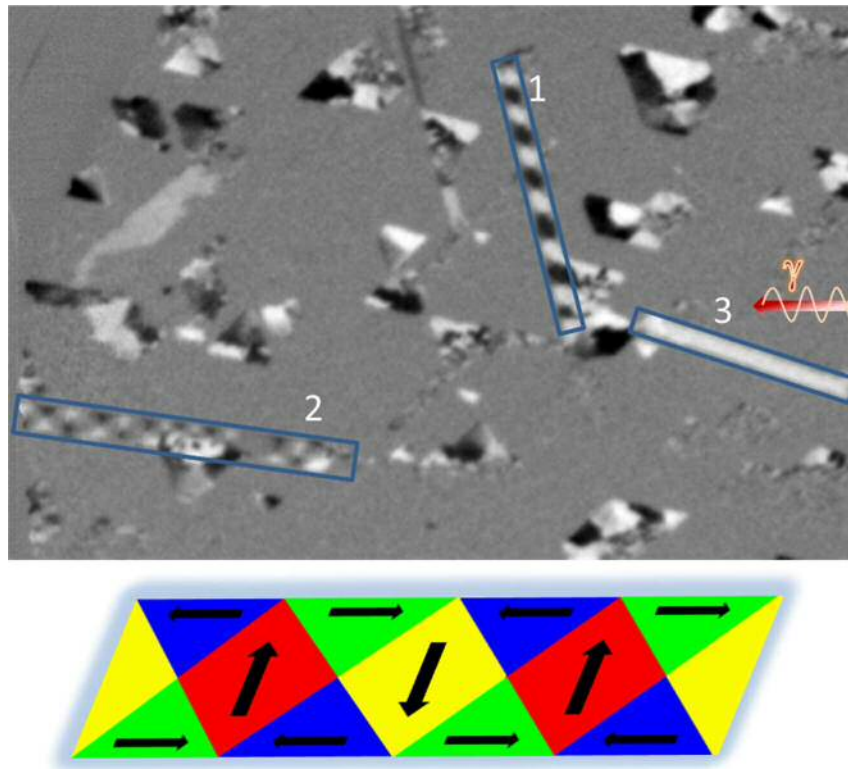


Figure 1. XMCD-PEEM image (field-of-view $11 \mu\text{m} \times 7 \mu\text{m}$) at the Fe L_3 -edge obtained at RT in the initial state. Incoming photon direction indicated by red arrow.

Heating the sample above $250 \text{ }^\circ\text{C}$, we confirmed the transition as a function of temperature, identifying specific strips that were observed to be in single-domain state at RT and diamond state at $250 \text{ }^\circ\text{C}$ (results not shown).

Fig. 2a presents an XMCD-PEEM image of the same area depicted in Fig. 1 after extracting the sample out of the UHV microscope chamber and exposing it to air for 30 mins. The Fe strips are seen to remain magnetic after exposure to air, in particular the **first** and third wire described in the context of Figure 1 are found to be in the same domain configuration (strip “1” in diamond pattern, strip “3” single domain, white). Subsequently, the sample was heated to $250 \text{ }^\circ\text{C}$ and another XMCD-PEEM image, shown in Fig. 2b, was collected.

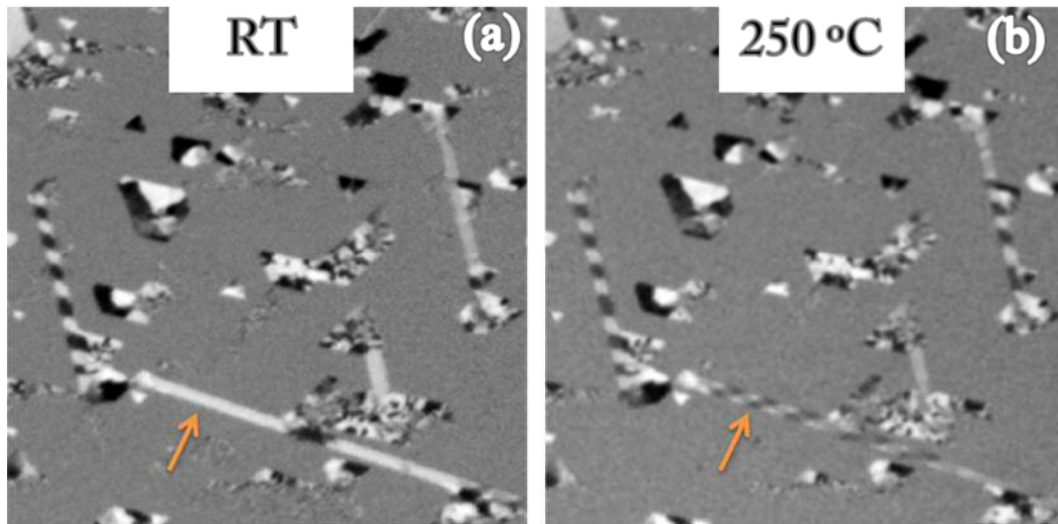


Figure 2. XMCD-PEEM images (field-of-view $9\ \mu\text{m} \times 9\ \mu\text{m}$) at the Fe L_3 -edge obtained at RT and 250 °C after exposing the Fe strips to air for 30 mins.

Remarkably, the transition from single-domain to multi-domain pattern is observed for the strip “3” indicated by the arrow in the same temperature range as before air exposure, i.e. between RT and 250 °C.[9] The transition temperature depends on the width of the wire, and is the consequence of a delicate balance between the magnetic anisotropies at play: magnetocrystalline, shape and magnetoelastic anisotropy.[9] The occurrence of the transition at very similar temperatures is an indication that this anisotropy balance is, at most, only mildly affected by air exposure. On the other hand, a closer examination of Fig. 2 seems to indicate that the magnetic contrast in the Fe strips is fainter at 250 °C than at RT. Fig. 3 shows the histogram of pixel intensities at both temperatures for strip 1, which confirms a 35% decay in pixel intensity asymmetry -and thus in magnetic contrast- between black and white magnetic domains, from 0.34 at RT to 0.22 (arbitrary units) at higher temperatures. Given that the two images were taken under identical experimental conditions, this 35% decrease in asymmetry implies a 35% decrease in the magnetization component of the Fe strip that is parallel to the incoming photon beam. The Curie temperature of Fe (770 °C) is well above the temperature range studied here (25-250 °C);

therefore such a considerable decay in magnetization cannot be explained by proximity to T_c . [11] In addition, the magnetic magnetite islands that surround the strips do not show a decrease in contrast (nor magnetization). This decrease in magnetization could be related to oxygen diffusion onto the bulk of the strip triggered by annealing and leading to a thicker non-magnetic surface layer. However, the inverse magnetostriction effect could be playing a role as well. Due to the difference in thermal expansion coefficients discussed in our previous work, it leads in this system to a cross-over in the anisotropy balance and ultimately governs the single to multi-domain transition. [9] The presence of magnetoelastic anisotropy could affect the magnetization component along the incident beam by either: 1. rotating the domain magnetization, or 2. a decrease of the saturation magnetization of the strips as a consequence of the strain-induced lattice change. [11]

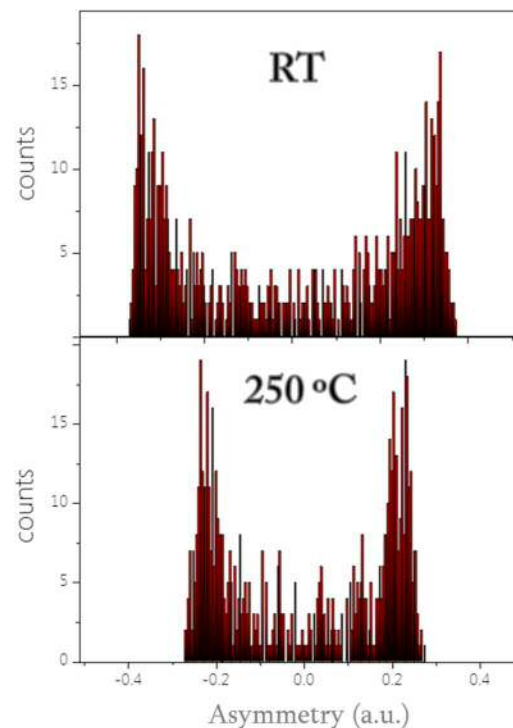


Figure 3. Pixel intensity asymmetry between black and white magnetic domains in Fe strips in the multi-domain state at RT and 250 °C. Histogram data for pixels of **strip 1** (not full image) obtained from the images in Fig. 2.

In order to further understand the extent of the effect of air exposure, PEEM images were obtained at different photon energies. By selecting the region of interest in the image, the XAS spectra of the strips were measured before and after air exposure. Fig. 4 depicts the corresponding spectra.

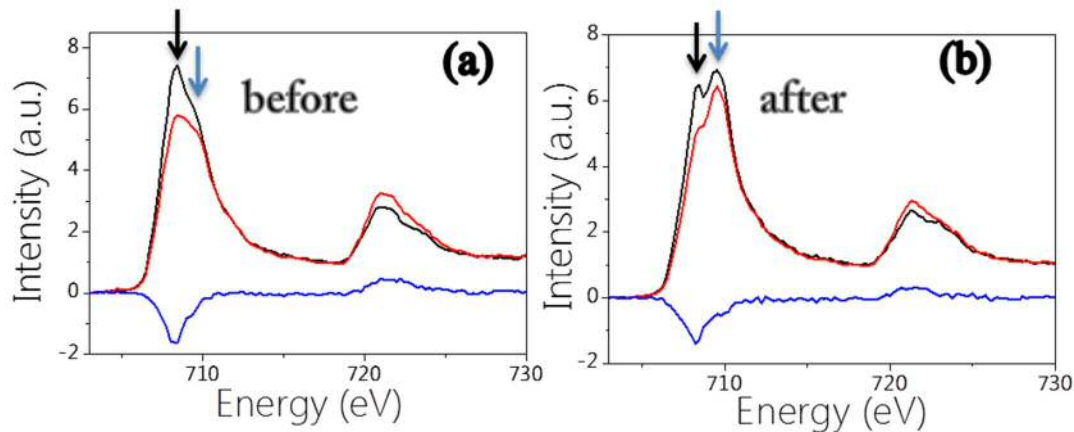


Figure 4. XAS spectra at the Fe L -edge obtained at RT before and after exposing the Fe strips to air for 30 mins. The spectra are obtained for the two opposite photon helicities (red and black curves). The resulting XMCD curve is shown in blue.

The L_3 -edge of the spectra before exposure presents a small shoulder at 709.6 eV (blue arrow) right after the L_3 edge itself at 708.3 eV (black arrow) that could be ascribed to a certain degree of oxidation of the Fe strips.[12,13] This observation is not surprising given that the sample was grown under 10^{-6} mbar of O_2 and that the strips are known to be capped by a thin FeO surface layer as a consequence.[9] However, in the XAS spectra after air exposure, the post-edge peak at 709.6 eV (blue arrow) becomes dominant in intensity, indicating a larger extent of the oxidation. A recent atomistic study using reactive molecular dynamics simulations concluded that the oxidation of the Fe(110) surface (the strips grow along the [110] direction) yields to the formation of a surface layer of Fe_2O_3 and a subsurface layer composed of FeO_{1-x} . [14] The XAS spectra after exposure is consistent with such a configuration.[13] Additionally, it is worth noting as well that the

XMCD signal presents a single peak as expected for metallic Fe, which is consistent with the coexistence of magnetic metallic Fe with non-magnetic oxides such as FeO and Fe₂O₃, as magnetite and maghemite portray a double XMCD peak at the *L₃-edge*. [12]

The thickness of this oxide layer has been estimated to be between 2-5 nm in recent theoretical and experimental studies; [14,15] thus, the strips under study here are inferred to be composed, after air exposure, of a metallic Fe bulk 20-30 nm thick (the thickness depends on the wire), capped with a 2 to 5 nm oxide layer of Fe₂O₃/ FeO_{1-x}.

From the XMCD spectra, and by applying the sum rules, [16] the spin and orbital magnetic moments of Fe were calculated before and after air exposure. The orbital moment decays from 0.1 to 0.09 μ_B whereas the spin moment varies from 1.17 to 0.94 μ_B upon air exposure. This 10% and 20% respective decrease in the values of the magnetic moments can be explained by the increase of non-magnetic Fe cations hosted by the surface oxide species after exposure, as they contribute to the XAS spectra but not to the XMCD signal.

4. Conclusions.

The single to multi-domain transition present in Fe strips grown on Ru(0001) remains unaltered after exposing the nanostructures to ambient conditions for 30 mins. The thin FeO layer existing at the surface of the wires after growth oxidizes partially to Fe₂O₃ and increases its thickness to 2-5 nm upon exposure. However, this oxide surface layer prevents further oxidation of the bulk of the Fe strips thus remarkably preserving the magnetic properties up to the exposure time investigated in this work, in particular the delicate balance of anisotropies that governs the transition. The results presented in this work enable avoiding the use of capping layers and increase in general the applicability of this effect in memory devices.

Acknowledgments:

This work is supported by the Spanish Ministry of Economy and Competitiveness through Projects No. MAT2015-64110-C2-1-P, MAT2015-64110-C2-2-P and MAT2013-48009-C4-1-P and the European Commission through the project NANOPYME FP7-NMP-2012-SMALL-6 NANOPYME (Grant No. 310516). These experiments were performed at the CIRCE beamline of the ALBA Synchrotron Light Facility with the collaboration of ALBA staff.

References:

- [1] R.L. Stamps, S. Breitzkreutz, J. Åkerman, A. V Chumak, Y. Otani, G.E.W. Bauer, et al., The 2014 Magnetism Roadmap, *J. Phys. D. Appl. Phys.* 47 (2014) 333001.
- [2] A. Hirohata, H. Sukegawa, H. Yanagihara, I. Zutic, T. Seki, S. Mizukami, et al., Roadmap for Emerging Materials for Spintronic Device Applications, *IEEE Trans. Magn.* 51 (2015) 1–11. doi:10.1109/TMAG.2015.2457393.
- [3] L. Martín-García, A. Quesada, C. Munuera, J.F. Fernández, M. García-Hernández, M. Foerster, et al., Atomically Flat Ultrathin Cobalt Ferrite Islands, *Adv. Mater.* 27 (2015) 5955. doi:10.1002/adma.201502799.
- [4] S. Farokhipoor, C. Magen, S. Venkatesan, J. Iniguez, C.J.M. Daumont, D. Rubi, et al., Artificial chemical and magnetic structure at the domain walls of an epitaxial oxide, *Nature.* 515 (2014) 379–383.
- [5] S. Mangin, M. Gottwald, C.-H. Lambert, D. Steil, V. Uhlíř, L. Pang, et al., Engineered materials for all-optical helicity-dependent magnetic switching, *Nat Mater.* 13 (2014) 286–292.

- [6] C.F. Vaz, J.C. Bland, G. Lauhoff, Magnetism in ultrathin film structures, *Reports Prog. Phys.* 71 (2008) 56501. doi:10.1088/0034-4885/71/5/056501.
- [7] B. Santos, S. Gallego, A. Mascaraque, K.F. McCarty, A. Quesada, A.T. N'Diaye, et al., Hydrogen-induced reversible spin-reorientation transition and magnetic stripe domain phase in bilayer Co on Ru(0001), *Phys. Rev. B - Condens. Matter Mater. Phys.* 85 (2012) 3–8. doi:10.1103/PhysRevB.85.134409.
- [8] F. El Gabaly, K.F. McCarty, A.K. Schmid, J. De La Figuera, M.C. Muñoz, L. Szunyogh, et al., Noble metal capping effects on the spin-reorientation transitions of Co/Ru(0001), *New J. Phys.* 10 (2008). doi:10.1088/1367-2630/10/7/073024.
- [9] A. Quesada, M. Monti, I.P. Krug, N. Rougemaille, F. Nickel, D.M. Gottlob, et al., Reversible temperature-driven domain transition in bistable Fe magnetic nanostrips grown on Ru(0001), *Phys. Rev. B.* 92 (2015) 24416. doi:10.1103/PhysRevB.92.024416.
- [10] L. Aballe, M. Foerster, E. Pellegrin, J. Nicolas, S. Ferrer, The ALBA spectroscopic LEEM-PEEM experimental station: layout and performance, *J. Synchrotron Radiat.* 22 (2015).
- [11] B.D. Cullity, C.D. Graham, Ferromagnetism, in: *Introd. to Magn. Mater.*, John Wiley & Sons, Inc., 2008: pp. 115–149. doi:10.1002/9780470386323.ch4.
- [12] E. Pellegrin, M. Hagelstein, S. Doyle, H.O. Moser, J. Fuchs, D. Vollath, et al., Characterization of Nanocrystalline γ -Fe₂O₃ with Synchrotron Radiation Techniques, *Phys. Status Solidi.* 215 (1999) 797–801. doi:10.1002/(SICI)1521-3951(199909)215:1<797::AID-PSSB797>3.0.CO;2-D.
- [13] M. Monti, B. Santos, A. Mascaraque, O. Rodríguez de la Fuente, M.A. Niño, T.O.

- Mentes, et al., Oxidation Pathways in Bicomponent Ultrathin Iron Oxide Films, *J. Phys. Chem. C.* 116 (2012) 11539–11547.
- [14] R. Subbaraman, S.A. Deshmukh, S.K.R.S. Sankaranarayanan, Atomistic Insights into Early Stage Oxidation and Nanoscale Oxide Growth on Fe (100), Fe (111) and Fe (110) Surfaces, *J. Phys. Chem. C.* 117 (2013) 5195–5207.
- [15] T.D. Ta, A.K. Tieu, H. Zhu, B. Kosasih, Adsorption of Normal-Alkanes on Fe (110), FeO (110), and Fe₂O₃ (0001): Influence of Iron Oxide Surfaces, *J. Phys. Chem. C.* 119 (2015) 12999–13010. doi:10.1021/acs.jpcc.5b01847.
- [16] C.T. Chen, Y.U. Idzerda, H.-J. Lin, N. V Smith, G. Meigs, E. Chaban, et al., Experimental Confirmation of the X-Ray Magnetic Circular Dichroism Sum Rules for Iron and Cobalt, *Phys. Rev. Lett.* 75 (1995) 152–155.
doi:10.1103/PhysRevLett.75.152.